

Diffusion enhanced carbon loss from SiGeC layers due to oxidation

M. S. Carroll*

Agere Systems, 600 Mountain Avenue, Murray Hill, New Jersey 07974

J. C. Sturm

Department of Electrical Engineering, Princeton University, Princeton, New Jersey 08544

E. Napolitani, D. De Salvador, and M. Berti

INFN and Department of Physics, University of Padova, Padova, Italy

J. Stangl and G. Bauer

Institute for Semiconductor Physics, Johannes-Kepler University Linz, Linz, Austria

D. J. Tweet

Sharp Laboratories of America, 5700 NW Pacific Rim Boulevard, Camas, Washington 98607

(Received 2 January 2001; published 31 July 2001)

The effect of annealing 25-nm-thick pseudomorphic $\text{Si}_{0.7865}\text{Ge}_{0.21}\text{C}_{0.0035}$ layers on silicon substrates in nitrogen or oxygen at 850 °C was examined for different silicon cap thicknesses and annealing times by x-ray diffraction and secondary-ion mass spectrometry. Carbon is found to diffuse rapidly out of the SiGeC layer and even out of the sample entirely, an effect that is enhanced by oxidation and thin cap layers. All substitutional carbon can be removed from the sample in some cases, implying negligible formation of silicon-carbon complexes. Furthermore, it is found that each injected silicon interstitial atom due to oxidation causes the removal of one additional carbon atom for the SiGeC layer.

DOI: 10.1103/PhysRevB.64.073308

PACS number(s): 66.30.Jt

Substitutional carbon incorporation in silicon and SiGe has drawn significant attention due to its ability to consume silicon interstitials, which mediate boron diffusion.¹ However, the potential that the interstitial-carbon product is a defect (i.e., β -SiC precipitation or carbon clusters)^{2,3} may limit the usefulness of carbon for diffusion engineering. Previous studies of carbon thermal stability in SiGeC confirm that the carbon can precipitate in SiGeC.^{2,4} In this report carbon out-diffusion from thin SiGeC layers is examined and is found to be the dominant mechanism of carbon loss for samples close to the surface, even in the regime of carbon concentration far above solid solubility or in the presence of excess interstitials injected during oxidation.

Two test structures with 25-nm-thick $\text{Si}_{0.7865}\text{Ge}_{0.21}\text{C}_{0.0035}$ layers capped by 50 or 280 nm of silicon were grown by rapid thermal chemical vapor deposition (RTCVD) at temperatures between 625 and 750 °C using dichlorosilane, germane, and methylsilane as the silicon, germanium, and carbon sources, respectively.⁵ Each test structure was grown on a *p*-type Czochralski (CZ) (100) silicon wafer.

Samples of the as-grown and annealed structures were examined using secondary-ion mass spectrometry (SIMS), which were sputtered using 1–2-keV Cs^+ ions. Depths were determined using standard profilometry of the sputtered craters leading to a 5% uncertainty in depths, a 20% uncertainty in carbon concentrations, and approximately a 1–2% uncertainty in germanium concentrations.

All as-grown and annealed samples were examined by x-ray diffraction (XRD) using a double-crystal rocking-curve geometry around the (004) Bragg reflection. Rocking curves of as-grown and oxidized samples were fitted by simulations

and agreed well with germanium and carbon profiles obtained by SIMS, indicating that the carbon in the SiGeC layer compensated the strain as if it was all substitutional, within the uncertainty of the measurement. The strain compensation relationship between germanium and carbon used was 12:1.⁶ As-grown and 960-min nitrogen or oxygen annealed samples of the 280-nm Si-capped structures were also examined for relaxation in the plane parallel to the growth surface by scanning around the (224) Bragg reflection. No relaxation was observed.

Carbon profiles from samples of the 280-nm silicon-capped structure annealed in nitrogen ambient for 240 or 960 min are overlaid on the as-grown carbon profile, Fig. 1(a). The appearance of carbon tails, indicative of carbon out-

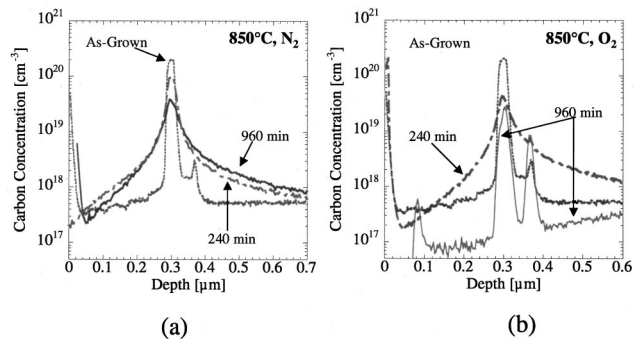


FIG. 1. Carbon concentration profiles from samples of the structure with a 280-nm silicon-capped SiGeC layer before and after annealing at 850 °C in (a) nitrogen or (b) oxygen ambient for 240–960 min overlaid on the as-grown carbon profile.

diffusion, is observed after annealing. Carbon diffusion in silicon is believed mediated by a combined interstitial kick-out [Eq. (1)] and the energetically less favorable Frank-Turnbull [Eq. (2)] mechanism,⁷



where C_s is a carbon atom in a substitutional site, I is the silicon interstitial, C_i is the mobile interstitial carbon defect, and V is a silicon vacancy. The distinct non-Gaussian broadening of the carbon profiles after nitrogen annealing has been explained as a result of a depleted interstitial concentration in the carbon-rich region, presumably because the kick-out mechanism is so rapid that it produces an undersaturation of interstitials locally. Because the interstitial population is depleted in the carbon region, a “stationary” profile is observed surrounded by tails of carbon “kicked-out” by the transport-limited diffusion of interstitials from the surrounding silicon.⁷ The asymmetry of the carbon profiles after annealing, i.e., lower carbon concentrations on the surface side of the SiGeC layer, indicates that there is carbon loss from the sample due to carbon diffusion towards and out the surface. Previous studies have also reported loss of carbon from slightly carbon enriched ($8 \times 10^{17} \text{ cm}^{-3}$) crystalline silicon out the surface after annealing in either oxygen or nitrogen ambient.⁸

The rate of carbon loss from the SiGeC layer is enhanced by oxidation, Fig. 1(b), and the carbon is reduced well below the as-grown background concentration ($3 \times 10^{17} \text{ cm}^{-3}$) except two spikes of immobile carbon after 960 min of oxidation located at 300 and 370 nm. The oxide-silicon interface is indicated by the carbon spike located at a depth of 100 nm in this sample. The carbon spike located outside the SiGeC layer at 370 nm depth in the as-grown sample, Figs. 1(a) and 1(b), was unintentional and is centered at the same location as a buried 15-nm-wide boron layer with a peak concentration of $4 \times 10^{18} \text{ cm}^{-3}$, suggesting that boron might promote immobile carbon complexing. Because the amount of carbon in these immobile layers is small, their effect on the quantification of carbon loss from the sample and SiGeC layer is ignored for the rest of the paper.

In Fig. 2(a) the carbon concentration profiles of the as-grown structure with a 50-nm Si cap and the samples annealed for 30 or 120 min in nitrogen ambient are shown. The peak carbon concentration is approximately half the as-grown concentration after 120 min of annealing without significant broadening of the carbon profile implying that carbon leaves the SiGeC layer and the sample entirely. Presumably the primary mechanism of loss is diffusion to the surface and the carbon tails are obscured by the higher carbon detection limits ($3 \times 10^{18} \text{ cm}^{-3}$). The carbon concentration profiles after oxidation of 30 to 120 min, Fig. 2(b), show a more rapid decrease of the carbon concentration, resulting in no detectable carbon in this sample after 120 min of oxidation.

Immobile carbon in the SiGeC layer is observed in the layers capped with a 280-nm silicon cap but not in the SiGeC layers capped by 50 nm of silicon although the initial germa-

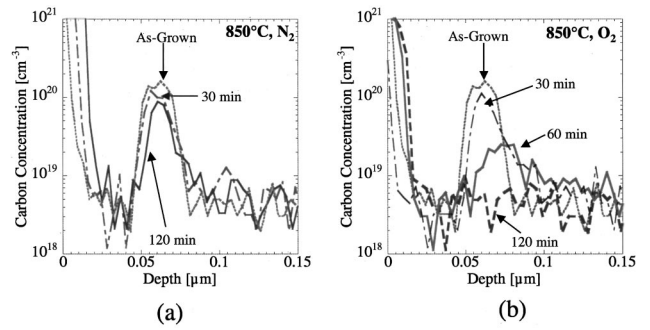


FIG. 2. Carbon concentration profile from samples of the structure with a 50-nm silicon-capped SiGeC layer before and after annealing at 850 °C in (a) nitrogen or (b) oxygen ambient for 30–120 min overlaid on the as-grown carbon profile.

nium and carbon concentrations are nearly identical. The formation of immobile carbon in the SiGeC layer with a 50-nm Si cap is, perhaps, prevented by the rapid carbon out-diffusion to the surface and surrounding silicon compared to that from the layer with the thicker 280-nm Si cap. Previous reports of carbon precipitation or immobile carbon are typically from much thicker carbon layers in silicon or SiGeC.^{2–4} In these cases the carbon concentration in the middle of the layer remains near the as-grown value longer because the carbon out-diffusion is predominantly at the edges of the layers. Indeed, transmission electron microscopy (TEM) measurements of thin SiC layers annealed in nitrogen for similar times as in this study showed no signs of precipitates.⁹ The formation of immobile carbon in the SiGeC layer due to the presence of boron is also possible; however, the boron concentration throughout all annealing times was less than $5 \times 10^{17} \text{ cm}^{-3}$ within the SiGeC layer, 100 times less than the final immobilized carbon.

To quantify the loss of carbon from the SiGeC layer and from the sample, the total carbon detected by SIMS in the SiGeC layers (circles) or in all of the sample (squares) after annealing in either nitrogen (solid symbols) or oxygen (open symbols) is subtracted from the carbon measured in the as-grown samples for both structures with Si caps of 50 and 280 nm in Figs. 3(a) and 3(b), respectively. The extra carbon lost due to oxidation begins to dominate only after longer oxidation times in both samples; however, clearly the carbon loss from the 280-nm Si capped SiGeC layer is significantly slower. The two different rates of oxidation-enhanced carbon loss, carbon lost after oxidation subtracted from that lost after annealing in nitrogen, from the 50-nm Si capped (circles) or 280-nm Si capped (squares) structures, is shown in Fig. 4. Clearly, oxidation removes significantly more carbon from the 50-nm Si-capped SiGeC layer than from the 280-nm Si-capped SiGeC layer after the same oxidation time.

Oxidation is known to inject interstitials into the silicon bulk at the surface and the enhanced carbon diffusion and carbon loss from the SiGeC layers after oxidation qualitatively can be explained by an increase in mobile carbon, C_i , due to the injected interstitials. SiGeC layers are reported as near-perfect interstitial sinks for all interstitials injected during oxidation for layers containing similar atomic compositions as those in this work.¹⁰ Therefore the additional in-

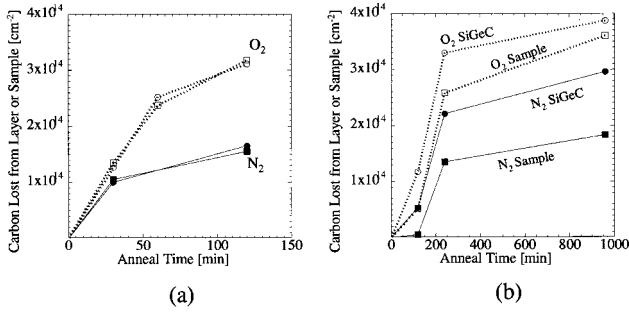


FIG. 3. Summary of total carbon lost from the SiGeC layer (circles) or the entire sample (squares) of the (a) 50 nm and (b) 280 nm Si-capped layers, after annealing in either oxygen (open symbols) or nitrogen (solid symbols) ambient at 850 °C.

jected interstitials are expected to “kick-out” a similar number of carbon, since all injected interstitials are consumed at the SiGeC layer.

During oxidation the surface concentration of interstitials is constant,¹¹ resulting in a linearly decaying interstitial profile from the surface supersaturation concentration to approximately zero at the SiGeC layer.^{12,13} The interstitial flux into the silicon during oxidation can therefore be calculated as

$$J_I = -D_I \frac{dI}{dx} = n_{\text{surf}} \frac{D_I I^*}{\Delta x}, \quad (3)$$

where n_{surf} is the ratio of the interstitial surface concentration to the bulk interstitial concentration (I/I^*), $D_I I^*$ is the interstitial transport product measured by metal tracer diffusion,¹⁴ and dx is the depth of the SiGeC layer. The total number of injected interstitials after oxidation is calculated as the time integrated flux and is compared to the extra carbon that leaves the SiGeC layer due to oxidation for the 50-nm Si-capped (dashed line) and 280-nm Si-capped (dotted) struc-

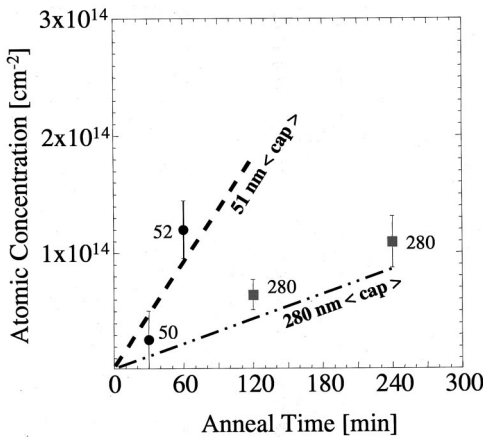


FIG. 4. Summary of oxidation-enhanced carbon loss from the SiGeC layer. The difference of carbon lost between oxidation and nitrogen anneals is shown for the 50-nm Si-capped (circles) and 280-nm Si-capped (squares) layers. The number of injected interstitial silicon atoms after oxidation is also calculated for the 50-nm Si-capped (dashed line) and 280-nm Si-capped (dotted line) layers.

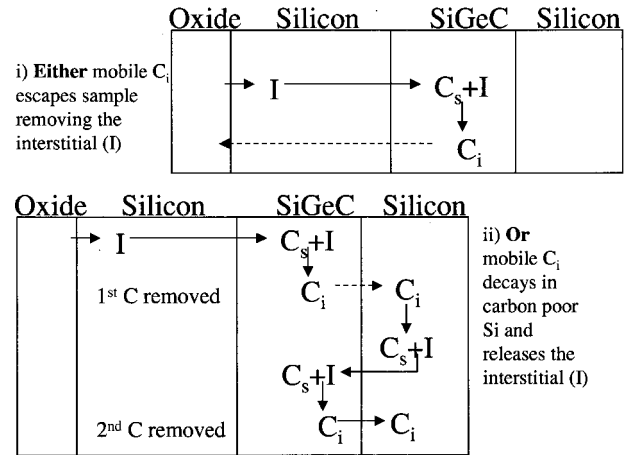


FIG. 5. Schematic diagram of interstitial recycling.

tures (Fig. 4). The Si cap thickness measured with SIMS is shown beside the carbon loss value for each structure.

The calculated number of interstitials injected into the 50-nm Si-capped SiGeC layer is nearly identical to the extra carbon that diffuses out of the SiGeC layer due to oxidation (Fig. 4) after 30- and 60-min annealing [the value for 60 min was interpolated from the nitrogen data in Fig. 3(a)]. After 120 min the measured oxidation enhancement saturates and diverges from the calculated interstitial injection because the carbon, by this time, is entirely removed from the SiGeC layer. Note: the calculated number of interstitials injected relied solely on the validity of Eq. (3), the $D_I I^*$ product from the literature ($1 \times 10^4 \text{ cm}^{-1} \text{ s}^{-1}$),¹⁴ typical interstitial supersaturations reported in the literature ($n_{\text{surf}} = 12.7$),^{11,13} and the depth of the layer. There were no adjustable variables available in this calculation.

Because the interstitial injection rate depends inversely on the depth of the SiGeC layer [Eq. (3)], the number of interstitials injected into the 280-nm Si-capped layer is less than that into the 50-nm Si-capped layer and therefore the oxidation-enhanced carbon diffusion is also smaller (Fig. 4). However, the number of interstitials injected into 280-nm Si-capped layer is actually less than the extra carbon removed from the SiGeC layer. Assuming carbon diffusion is described by the reactions in Eqs. (1) and (2) one interstitial migrating into the SiGeC layer can be responsible for the production of only a single mobile carbon. However, one additional interstitial injected at the surface may be responsible for the removal of multiple carbon from the SiGeC layer, if the mobile carbon that leaves the SiGeC layer decays back to a substitutional carbon and an interstitial in the surrounding silicon near the SiGeC layer. The interstitial is then free to migrate back to the SiGeC layer and remove a second carbon from the SiGeC layer (see Fig. 5), effectively recycling the interstitial, and therefore increasing the ratio of extra carbon removed to injected interstitials above unity. The amount of recycling will depend on the carbon layer proximity to the surface, because some mobile carbon will escape the sample via the surface removing the interstitial completely from the sample. As is indeed observed,

the ratio of injected interstitials to removed carbon is nearly 1:1 for the SiGeC layer closest to the surface and only diverges to greater than 1:1 for the deeper SiGeC layer. The observed 1:1 ratio also indicates that the carbon does not bind in clusters that can release more than one mobile carbon for a single injected interstitial, as might be expected if the carbon formed the well known C_s-C_i complex identified in other work.¹⁵

Carbon out-diffusion from $Si_{0.7865}Ge_{0.21}C_{0.0035}$ layers has been examined after annealing in nitrogen or oxygen

ambient at 850 °C. Carbon out-diffusion from the 25-nm-thick SiGeC layer is the dominant mechanism of carbon loss from the SiGeC layers with silicon caps of ≤ 280 nm. Carbon is found to diffuse out the surface and the carbon diffusion from the SiGeC layer is enhanced by oxidation. Each injected interstitial leads to a mobile carbon, which in turn may leave the sample if close to the surface or may lead to loss of multiple carbon from the SiGeC layer through the recycling process if the surface is further away.

This work was supported by ARO and DARPA.

*Electronic mail: malcarroll@agere.com

- ¹P. A. Stolk, H.-J. Gossmann, D. J. Eaglesham, D. C. Jacobson, J. M. Poate, and H. S. Luftmann, *Appl. Phys. Lett.* **66**, 568 (1995).
- ²P. Warren, J. Mi, F. Overney, and M. Dutoit, *J. Cryst. Growth* **157**, 414 (1995).
- ³J. W. Strane, H. J. Stein, S. R. Lee, S. T. Picraux, J. K. Watanabe, and J. W. Mayer, *J. Appl. Phys.* **76**, 3656 (1994).
- ⁴L. V. Kulik, D. A. Hits, M. W. Dashiell, and J. Kolodzey, *Appl. Phys. Lett.* **72**, 1972 (1998).
- ⁵J. C. Sturm, P. V. Schwartz, E. J. Prinz, and H. Manoharan, *J. Vac. Sci. Technol. B* **9**, 2011 (1991).
- ⁶D. De. Salvador, M. Petrovich, M. Berti, F. Romanato, E. Napolitani, A. Drigo, J. Stangl, S. Zerlauth, M. Muehlberger, F. Schaeffler, G. Bauer, and P. C. Kelires, *Phys. Rev. B* **61**, 13005 (2000).
- ⁷R. F. Scholz, P. Werner, U. Gosele, and T. Y. Tan, *Appl. Phys. Lett.* **74**, 392 (1999).
- ⁸L. A. Ladd and J. P. Kalejs, in *Oxygen, Carbon, Hydrogen, and Nitrogen in Crystalline Silicon*, edited by Mikkelsen, and Pearton, Corbett, Pennycook, Mater. Res. Soc. Symp. Proc. No. 59 (Materials Research Society, Pittsburgh, PA, 1986), p. 445.
- ⁹P. Werner, H.-J. Gossmann, D. C. Jacobson, and U. Gösele, *Appl. Phys. Lett.* **73**, 2465 (1998).
- ¹⁰M. S. Carroll, C.-L. Chang, J. C. Sturm, and T. Buyuklimanli, *Appl. Phys. Lett.* **73**, 3695 (1998).
- ¹¹S. T. Dunham, *J. Appl. Phys.* **71**, 685 (1992).
- ¹²M. S. Carroll and J. C. Sturm, in *Silicon Front-End Processing—Physics and Technology of Dopant-Defect Interactions II*, edited by A. Agarwal, L. Pelaz, H-H. Vuong, P. Packan, and M. Kase, Mater. Res. Soc. Symp. Proc. No. 610, B4.10, 2000 and www.mrs.org/publications/epubs/proceedings/spring2000/b/.
- ¹³M. S. Carroll, J. C. Sturm, and T. Buyuklimanli, *Phys. Rev. B* (to be published).
- ¹⁴H. Bracht, N. Stolwijk, and H. Mehrer, *Phys. Rev. B* **52**, 16 542 (1995).
- ¹⁵G. Davies and R. C. Newman, in *Handbook on Semiconductors*, edited by T. S. Moss (Elsevier, Amsterdam, 1994), p. 1558.